

RESEARCH ARTICLE

10.1002/2017JA024703

Key Points:

- Simultaneous occurrence of downward and westward nocturnal equatorial ionospheric plasma drifts during the 17 March 2015 geomagnetic storm
- Vertical and zonal plasma drifts exhibited distinct bipolar type variations
- In addition to storm time electric fields, storm induced local electrodynamic changes are found to be responsible for these drift features

Correspondence to:

M. S. Bagiya,
bagiyamala@gmail.com;
mala@iigs.iigm.res.in

Citation:

Bagiya, M. S., Vichare, G., Sinha, A. K., & Sripathi, S. (2018). On the nocturnal downward and westward equatorial ionospheric plasma drifts during the 17 March 2015 geomagnetic storm. *Journal of Geophysical Research: Space Physics*, 123, 1618–1626. <https://doi.org/10.1002/2017JA024703>

Received 22 AUG 2017

Accepted 27 JAN 2018

Accepted article online 5 FEB 2018

Published online 24 FEB 2018

On the Nocturnal Downward and Westward Equatorial Ionospheric Plasma Drifts During the 17 March 2015 Geomagnetic Storm

Mala S. Bagiya¹ , Geeta Vichare¹, A. K. Sinha¹ , and S. Sripathi¹ ¹Indian Institute of Geomagnetism (DST), Navi Mumbai, India

Abstract During quiet period, the nocturnal equatorial ionospheric plasma drifts eastward in the zonal direction and downward in the vertical direction. This quiet time drift pattern could be understood through dynamo processes in the nighttime equatorial ionosphere. The present case study reports the nocturnal simultaneous occurrence of the vertically downward and zonally westward plasma drifts over the Indian latitudes during the geomagnetic storm of 17 March 2015. After ~17:00 UT (~22:10 local time), the vertical plasma drift became downward and coincided with the westward zonal drift, a rarely observed feature of low latitude plasma drifts. The vertical drift turned upward after ~18:00 UT, while the zonal drift became eastward. We mainly emphasize here the distinct bipolar type variations of vertical and zonal plasma drifts observed around 18:00 UT. We explain the vertical plasma drift in terms of the competing effects between the storm time prompt penetration and disturbance dynamo electric fields. Whereas, the westward drift is attributed to the storm time local electrodynamic changes mainly through the disturbance dynamo field in addition to the vertical Pedersen current arising from the spatial (longitudinal) gradient of the field aligned Pedersen conductivity.

Plain Language Summary The low latitude electrodynamic during geomagnetically disturbed period is significantly different as compared to that during the quiet period, which eventually affects the ionospheric plasma drifts by varying the ambient electric fields from that of its quiet time pattern. During nighttime, the low latitude plasma drifts vertically downward and zonally eastward under the effects of the ambient westward and downward electric fields, respectively. The present case study brings out a rarely observed feature of the nighttime equatorial plasma drifts, where the downward vertical drift coincided with the westward zonal drift during the geomagnetic storm of 17 March 2015. The storm time prevailing electric fields and the storm induced local electrodynamic changes are found to be responsible for this peculiar drift behavior.

1. Introduction

The most intense storm of the solar cycle 24, till date, occurred with two-step main phase on 17 March 2015. The first moderate step-I, which occurred with minimum symmetric ring current index (SYM-H) of ~ -101 nT at ~9:38 UT, was followed by the intense step-II with minimum SYM-H of ~ -234 nT at ~23:00 UT. Since this is the first strongest storm after a prolonged geomagnetic quiet period, it has received conspicuous attention from various scientific groups including the scientific community working in the field of equatorial and low latitude ionosphere. The observational studies pertaining to the effects of this storm on the global as well as regional ionosphere-thermosphere system are well documented since then (e.g., Astafyeva et al., 2015; Bahera et al., 2017; Carter et al., 2016; Kalita et al., 2016; Liu et al., 2016; Nava et al., 2016; Ramsingh et al., 2015; Ray et al., 2017; Zakharenkova et al., 2016; Zhang et al., 2015; Zhong et al., 2016). It has to be noted that main phase step-II of this storm coincided with the dusk to dawn period over the Indian region. Thus, it has provided a good opportunity to study the unique effects of this storm on the nocturnal low latitude ionospheric electrodynamic and concurrent plasma irregularities over the Indian longitudes (e.g., Patra et al., 2016).

During geomagnetic storm, the low latitude ionospheric electrodynamic is mainly controlled by the prompt penetration of dawn to dusk interplanetary electric field (IEFy) and delayed penetration of disturbance dynamo electric (DDE) field induced by the storm time disturbance wind. The IEFy penetrates instantaneously from high to low latitudes during southward interplanetary magnetic field (IMF) conditions (e.g., Fejer &

Emmert, 2003; Kelley et al., 2003; Nishida, 1968, and references therein). This prompt penetration electric (PPE) field manifests as eastward (dawn-to-dusk) electric field during daytime and westward (dusk-to-dawn) during the night. However, the delayed penetration of storm time wind induced DDE field manifests westward (eastward) during day (night) (e.g., Blanc & Richmond, 1980; Fejer, et al., 1983; Kelley & Retterer, 2008; Scherliess & Fejer, 1997, and references therein).

Nocturnal low latitude F region height variability is considered as good proxy for observing the storm time PPE field effects over the low latitudes in terms of vertical plasma drift variations (e.g., Bagiya et al., 2011; Patra et al., 2016; Ramsingh et al., 2015, and references therein). So far, as the penetration of meridional component of interplanetary electric field is concerned, very little is known due to its small amplitudes at low latitudes (cf. Abdu et al., 1998). Thus, the storm time zonal plasma drift is always the subject of great interest. During geomagnetically quiet period, the nighttime low latitude ionospheric plasma exhibits eastward drift in the zonal direction and downward in the vertical one under the effects of the downward and westward ambient electric fields, respectively (e.g., Fejer, 1993). The F region wind dynamo is mainly responsible for the eastward zonal drift, whereas the ambient westward electric field drives the plasma downward through $E \times B$ mechanism. These conventional drift variations deviate from its quiet time pattern when storm time electric fields superimpose over the ambient ionospheric electric fields. Abdu et al. (1998) studied the equatorial F region plasma drifts over the South Atlantic Magnetic Anomaly region during geomagnetic disturbances and emphasized the role of storm time low latitude ionospheric electrodynamics in varying these drifts. Fejer and Emmert (2003) reported storm time vertical and zonal plasma drift variations during the recovery phase of the geomagnetic storm of 19–21 October 1998 as observed from Jicamarca and Arecibo. Huang et al. (2010) showed vertical and zonal ion drifts over the equator during four large geomagnetic storms using DMSP F13 observations near the dusk sector. It has to be noted that Abdu et al. (1998), Fejer and Emmert (2003), and Huang et al. (2010) mostly report the storm time drift observations where upward plasma drift coincided with the westward zonal drift. Contrastingly, using ROCSAT-1 observations, Huang et al. (2008) showed the downward drift in simultaneity with westward drift during intense geomagnetic storms. However, in their study, they have not emphasized the simultaneous occurrence of these similar drift phases.

The present study reports the simultaneous nocturnal downward and westward plasma drifts during the geomagnetic storm of 17 March 2015 from the Indian dip equatorial station of Tirunelveli (8.73°N, 77.70°E; mag. 0.32°N). After ~17:00 UT (~22:10 LT) on 17 March 2015, the equatorial vertical plasma drift became downward and coincided with the westward plasma drift, which is a rarely observed feature of the low latitude plasma drifts. The vertical drift turned upward after ~18:00 UT, while the zonal drift became eastward. We emphasize here the distinct bipolar type variations of the plasma drifts observed around 18:00 UT. Not only we report this peculiar equatorial drifts behavior but also attempt to explain it in terms of competing effects between the storm time electrodynamical and neutral dynamical couplings as well as the storm induced local electrodynamical changes. Patra et al. (2016) presented the multitechnique observations of nighttime plasma drifts from the Indian low latitude station Gadanki (13.5°N, 79.2°E; mag. 6.3°N) during the same storm, but they have not discussed anything related to the simultaneous presence of downward and westward plasma drifts. Moreover, they presented the vertical drift till 14:30 UT, while our report pertains to the drift variations after 17:00 UT.

2. Data and Techniques

The halo coronal mass ejection that occurred on 15 March 2015 arrived at the Earth on 17 March at ~04:30 UT and conferred this intense storm (Kataoka et al., 2015). The storm is well studied by many researchers and the details can be found elsewhere (e.g., Kamide & Kusano, 2015; Kataoka et al., 2015). Here we present the storm condition through Figure 1 that shows the variations of IMF B_z and SYM-H during 17–18 March 2015. IMF B_z turned southward at ~6:00 UT on 17 March. The SYM-H variations imply that the storm main phase occurred in two steps (e.g., Kamide & Kusano, 2015). The period between 16:00 to 21:00 UT, which coincided with the premidnight to postmidnight hours over the Indian region, is of the prime interest here and thus marked with vertical lines in Figure 1. The IMF B_z and SYM-H index along with other interplanetary and high latitude ionospheric parameters, that is, IEFy, solar wind pressure, AL, and AU indices, for this marked temporal window are presented in Figure 2 to describe the disturbed condition in more detail during this period.

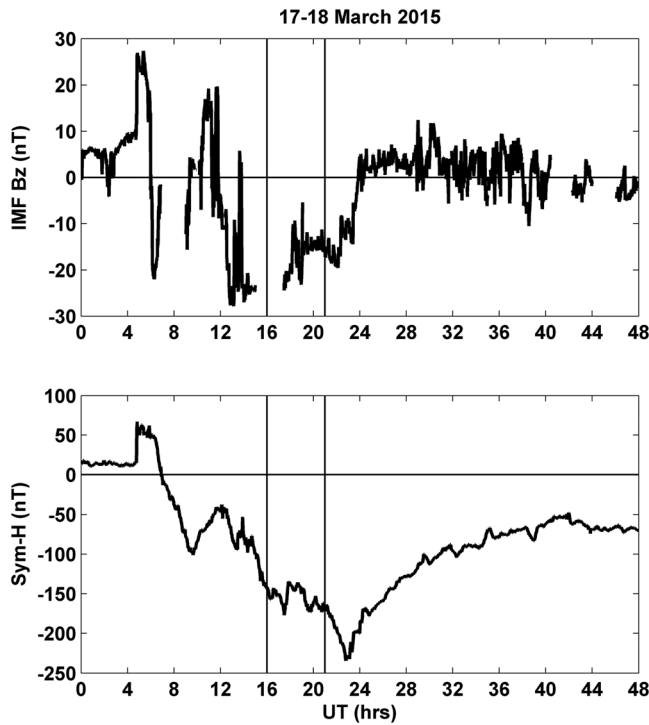


Figure 1. IMF B_z and SYM-H variations on 17–18 March 2015. From IMF B_z variations, it could be observed that storm initiated at $\sim 6:00$ UT on 17 March. The SYM-H observations imply that main phase occurred in two steps. The period of interest between 16:00 and 21:00 UT is highlighted with two vertical lines.

The co-located Canadian Advanced Digital Ionosonde (CADI) and spatially separated two L-band Global Navigation Satellite System (GNSS) receivers serve the main database for this study. The CADI is operational at Tirunelveli since 2006 and provides (a) the echo delay (virtual height) as a function of frequency, (b) the amplitude and phase of the reflected signal, and (c) the Doppler shift due to motion of the reflector at selected frequencies. It is an established diagnostic tool to study the climatological behavior of vertical and zonal plasma drifts over the equatorial region (e.g., Sripathi et al., 2016). The Doppler drift (both vertical and zonal) observations reported in the present study are recorded at 7 MHz frequency with 1 min time resolution in between two consecutive ionograms. More details on the functioning of CADI at Tirunelveli can be found in Sripathi et al. (2016).

Two GNSS receivers are recently installed at Tirunelveli to estimate the plasma irregularity zonal drift at L1-frequency. Assuming that L-band scintillation occurs at typical height of ~ 350 km, the first Fresnel zone at L1 ($\lambda = 19.05$ cm) can be given as $\sqrt{2\lambda h} = 365$ m (Iyer et al., 2006). In view of this, these receivers are placed east-west with spatial distance of ~ 376 m and observe the scintillation at L1-frequency signals from the Indian geostationary satellites (GSAT-8 and GSAT-10) in addition to other GNSS satellites. This setup uses the L-band scintillation patches as tracers to derive the nighttime irregularity zonal plasma drift. The cross correlation of the scintillation as recorded by both the receivers provides the magnitude of the drift.

3. Results

Figure 3a shows the vertical plasma drift (green circles) as estimated by CADI on the storm day during 16:00 to 21:00 UT. A minute interval mean drift is estimated using seven quiet days drift observations of the same month and presented in black scatter plot along with standard error bounds in Figure 3a. The Indian Standard Time (IST) scale is also mentioned in the figure for better visualization on LT variations of the drift. Large negative departure in vertical drift is observed at $\sim 17:50$ UT on 17 March. This negative swing is followed by positive upward rise, which, in general, remains absent on quiet days. The drift moves upward at $\sim 18:00$ UT and

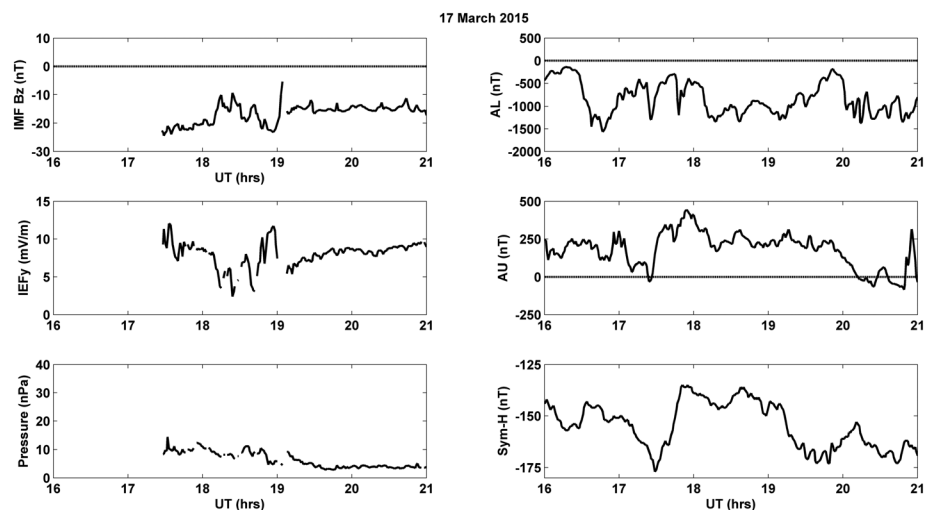


Figure 2. IMF B_z and SYM-H indices along with the IEFy, solar wind pressure, AL, and AU indices between 16 and 21 UT on 17 March to describe the highlighted period of Figure 1.

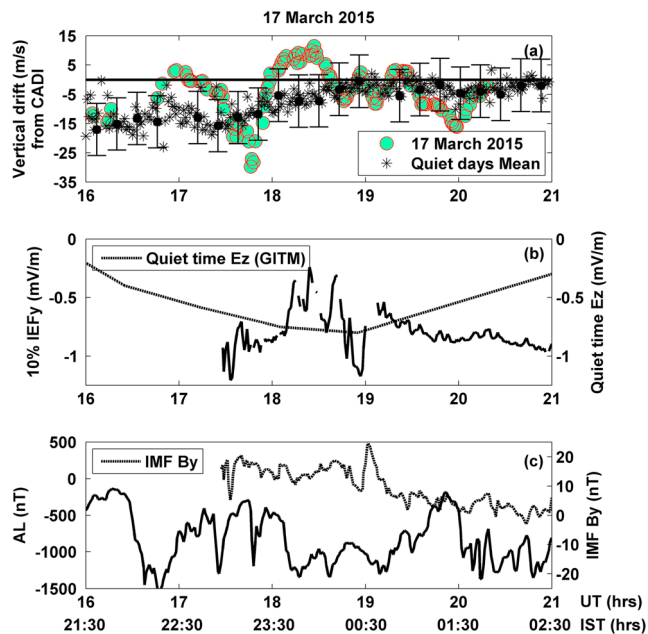


Figure 3. (a) Vertical plasma drift variations as observed by CADI from Tirunelveli on 17 March 2015 (green circles) during 16 to 21 UT. The black scattered plot shows the seven quiet days mean during March 2015 along with the error bounds. The positive (negative) values represent upward (downward) drift. (b) Prompt penetration induced zonal electric field, which is considered as 10% of the IEFy (solid line) along with the simulated quiet day ambient zonal field (dotted line) (Vichare et al., 2012). Since the study pertains to nighttime, negative (-ve) sign is introduced for IEFy. The enhanced downward drift at ~17:50 UT is attributed to the enhanced PPE field of ~-1.2 mV/m. (c) Variations in IMF B_y (dotted line) and AL index (solid line) during the period of interest.

remains positive till ~18:35 UT. Thereafter, it fluctuates up and down till 19:30 UT. However, these fluctuations are within the error bars of quiet days drift; thus, it is not logical to discuss it further. Significant downward drift is observed after 19:30 UT.

In order to understand the observed vertical drift, we estimate the prompt penetration induced zonal electric field, which is considered as 10% of the IEFy and the same has been presented in Figure 3b as solid line. It has been observed by many researchers that PPE field at the equatorial ionosphere is proportional to IEFy (e.g., Bhaskar & Vichare, 2013; Huang et al., 2007; Kelley et al., 1979; Nishida, 1968). However, estimation of the scaling factor between IEFy and equatorial ionospheric electric field is difficult (Fejer et al., 2007). Using empirical estimation, Huang et al. (2007) reported that the efficiency of penetration electric field in the dayside equatorial ionosphere is 9.6% of the IEFy. Whereas using Volland-Stern model, Burke (2007) found a theoretical penetration efficiency of 11.9%. Therefore, for present analysis we consider that 10% of IEFy penetrates to equatorial ionosphere, which is a reasonable approximation. Figure 3b also includes the ambient zonal electric field during quiet time (black dotted line). The quiet day ambient zonal field is taken from Vichare et al. (2012). They simulated this electric field at 300 km altitude over the magnetic equator using the Global Ionosphere-Thermosphere Model (GITM). More details on this can be found in Vichare et al. (2012). Quiet day zonal field remains stable westward throughout the period of interest. Since the study is confined to night time, negative (-ve) sign is introduced for IEFy in Figure 3b. On 17 March, the PPE field induced disturbance zonal field deviated significantly from the quiet time field and also exhibited fluctuations between 17:30 and 19:00 UT. Figure 3c represents the AL index and IMF B_y variations during this period and the same are discussed later.

The zonal plasma drift variations as obtained from spatially separated GNSS receivers and CADI Doppler techniques are showed in Figures 4a and 4b, respectively (blue circles), between 16:00 and 21:00 UT. The IST is also marked in the figure. The mean zonal drift is estimated from the seven quiet days drift observations and presented along with the standard error bounds in the respective figures. It could be noticed that the zonal plasma drift steadily decreased on quiet days but remained positive (eastward) throughout, as observed in both measurements. This drift behavior corroborates with the typical nighttime zonal drift as reported earlier (e.g., Bagiya et al., 2015; Fejer, 1993). On the storm day, the zonal drift decreased steadily till ~16:30 UT and then became westward. The westward zonal drift prevailed thereafter until it became eastward for a short period at ~18:00 UT as observed by CADI. The drift measurements are not available from L-band scintillation technique after 18:00 UT as the scintillation became weak. We intend to explain the observed downward and westward plasma drifts in purview of the storm time high latitude-low latitude ionospheric coupling and the resultant low latitude electrodynamic changes.

4. Discussion

It could be observed from Figure 3a that vertical drift attained maximum downward value (< -30 m/s) at ~17:50 UT. The PPE field induced zonal electric field was reduced to ~-1.2 mV/m at ~17:30 UT (Figure 3b). The zonal field could not be estimated earlier than 17:30 UT due to unavailability of the IEFy estimates. We presume here, that large downward vertical plasma drift after ~17:00 UT was due to the PPE field induced westward electric field over the equator. The time duration of 17:00–18:00 UT coincided with the sharp negative depressions in AL (onset of substorms) (Figure 3c). The injection of high energy particles during substorms changes the electric field shielding from high to low latitudes (e.g., Ahn et al., 1983).

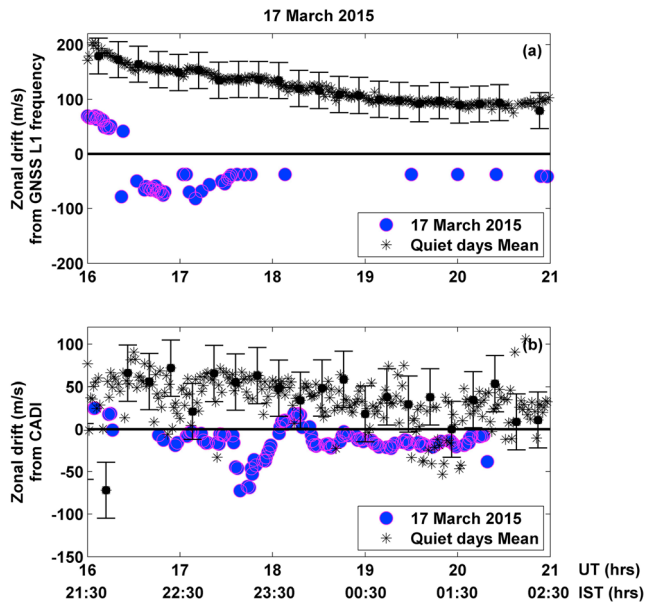


Figure 4. (a) Zonal plasma drift variations (blue circles) along with the mean of seven quiet days zonal drift (black scattered) as observed by spatially separated GNSS scintillation receiver technique during 16:00 to 21:00 UT. (b) The zonal drift as derived from CADI on the storm day (blue circles) and seven quiet days mean (black scattered). The positive (negative) values represent eastward (westward) drift. The drifts from both the observations show westward drift during ~16:30–18:00 UT that coincided with the downward plasma drift in Figure 3. The quiet days mean in both figures are shown with the error bars. From GNSS receiver technique, the drift measurements are not available after 18:00 UT. CADI measurements exhibited eastward drift for a short period of time after ~18:00 UT.

The role of magnetospheric electric field in causing the downward drift at ~17:50 UT could be verified from the high latitude convection pattern. Therefore, we present here (Figure 5) the Super Dual Auroral Radar Network (SuperDARN) (e.g., Greenwald et al., 1995) derived high latitude convection maps (source: <http://vt.superdarn.org>) for the selected time windows between 17:00 UT (~22:10 LT) and ~19:00 UT (~00:10 LT). The SuperDARN maps between 17:00 to 17:40 UT (Figures 5a and 5b) indicated the strengthening of convection cells at high latitudes; the convection has enhanced from 66 to 85 kV during this period. Hence, it is possible that the enhanced convection as shown by SuperDARN is associated with the enhanced PPE field through substorm onset as well as IEFy.

During this storm, the presence of nighttime DDE field (eastward) over the Indian longitudes has been reported extensively (e.g., Patra et al., 2016; Sau et al., 2017, and references therein). In particular, Sau et al. (2017) presented westward equatorial plasma bubble velocity between 16:00 and 21:00 UT using Airglow imager measurements from the same location of Tirunelveli and discussed in terms of the eastward manifestations of DDE field over the Indian longitudes. Therefore, despite the eastward DDE field, the observed vertical downward drift between 17:00 and 17:50 UT suggests the dominance of PPE field over the prevailing DDE field during this period.

The reduction in downward drift at ~18:00 UT could be associated with the reduction in PPE field. The drift turned upward after ~18:00 UT. The PPE field reduced after 18:00 UT (Figure 3b), and the decrease in convection was also evident from the SuperDARN maps (Figure 5c). This reduction leads to the weakening of downward drift. Thus, the observed upward turning of plasma drift could not be explained in terms of PPE field. We suggest that the prevailing eastward DDE field dominates the reduced PPE field effect and hence could be responsible for raising the vertical drift in upward direction.

Recently, Chakrabarty et al. (2017) reported the simultaneous presence of PPE induced eastward electric field at Thumba and Jicamarca. They explained this by emphasizing the role of IMF B_y directionality in controlling the convection cell movements at high latitudes, which affect the low latitude zonal electric field during a storm. In order to check the IMF B_y directionality in present case, IMF B_y variations for the specified time period are reproduced in Figure 3c. It is clear that IMF B_y is positive during the entire period of interest. In order to demonstrate the convection cell movements over the Tirunelveli LT sector, a line highlighting the LT corresponding to the respective UT is marked in SuperDARN maps (Figure 5). A careful investigation of Figure 5 revealed that the Tirunelveli LT sector falls in the dawn convection cell after 18:00 UT. The LT sector of Tirunelveli was deep into the dawn cell till 18:40 UT and could be verified from Figures 5d–5h. This might lead to eastward electric field penetration at low latitudes (e.g., Chakrabarty et al., 2017) and thereby augmenting the prevailing eastward DDE field during this period. However, considering the limited network of SuperDARN observations, the derived convection patterns during geomagnetic storms might not be reliable due to the statistical consideration. Significant downward drift observed at ~20:00 UT interestingly coincided with the substorm onset in AL (Figure 3c). We suggest that the PPE field associated with substorm onset at ~20:00 UT led to the downward drift around this period.

The storm time disturbances in dip equatorial zonal plasma drift, in the present case, are observed mainly as westward drift between 16:30 and 20:10 UT. Since the zonal plasma drift is linked to the vertical electric field, we wish to examine the vertical electric field during the addressed storm period. The meridional/vertical electric field penetration is not fully understood due to its very small amplitudes at low latitudes (cf. Abdu et al., 1998). In addition, direct measurements of vertical electric field are not available from the Indian low-latitude

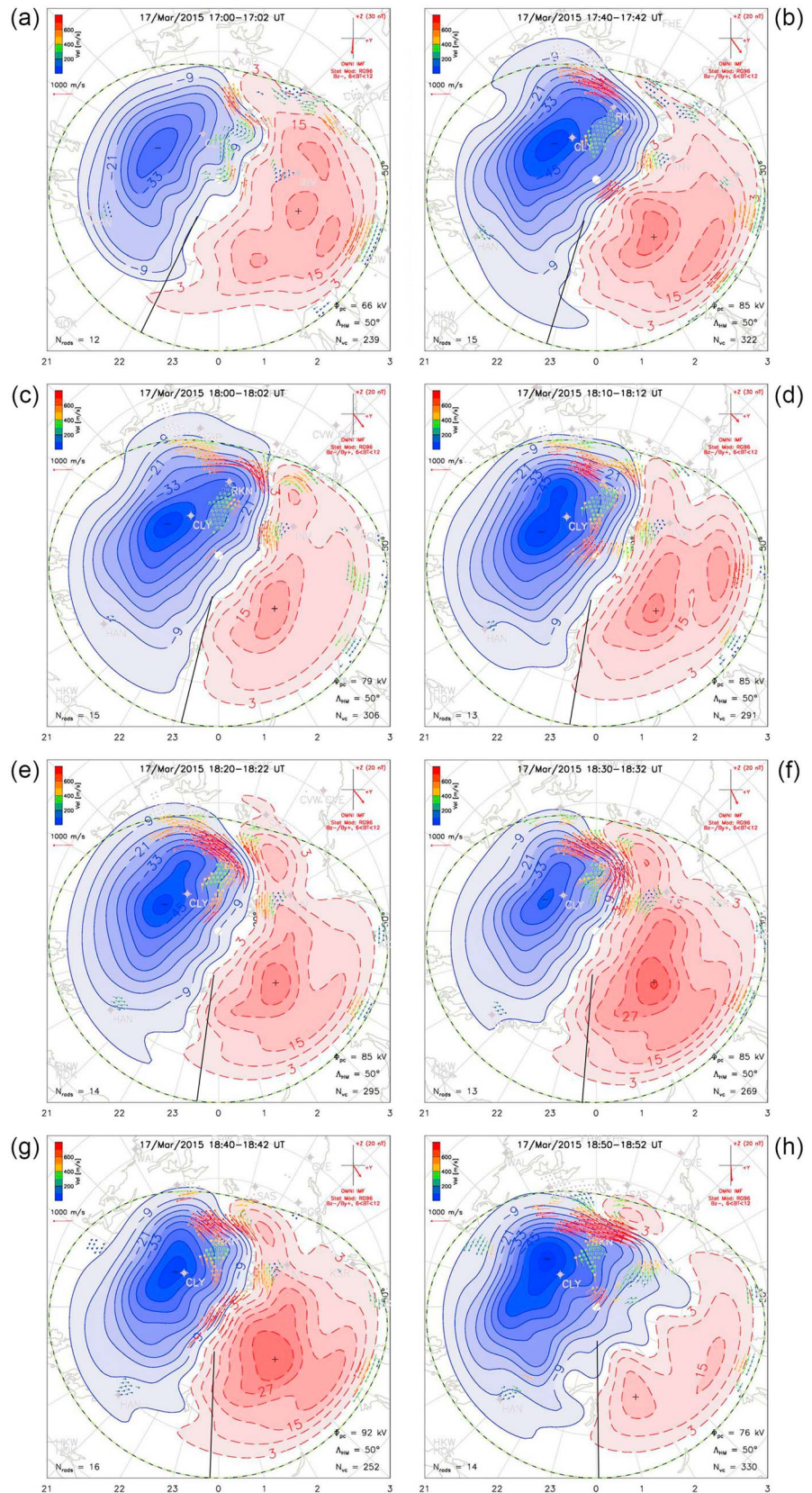


Figure 5. Ionospheric convection maps from SuperDARN along with DP2 contours during 17:00 to 18:52 UT for selected time windows. The local time sector of Tirunelveli for the given UT is shown with black solid line in each map.

region. Therefore, we estimate the vertical field using the mathematical expression proposed by Haerendel et al. (1992). According to this, the vertical electric field can be given as

$$E_V = \frac{\sum_H}{\sum_P} E_{EW} - BU_{EW}^P + \frac{J_V}{\sum_P} \quad (1)$$

The first term in the right hand side of equation (1) arises due to Hall conduction. Here, \sum_H and \sum_P are field-aligned Hall and Pedersen conductivities, E_{EW} is the zonal electric field. Storm time enhanced zonal electric field, if eastward, triggers the intense equatorial vertical plasma drift and also Hall electric field at low latitudes. This low latitude Hall field manifests as upward vertical field over the equatorial F region through mapping along the equipotential geomagnetic field lines, which ultimately affects equatorial zonal plasma drift (Abdu et al., 1998). Our empirical estimation based on the conductivities taken from IRI-2012 suggests that the ratio of $\frac{\sum_H}{\sum_P}$ is very small (~ 0.07) and the field contribution from the first term is ~ -1.02 mV/m (downward), during the period of simultaneous downward and westward plasma drifts.

The second term in the right hand side of equation (1) shows contribution from the wind dynamo. B is the geomagnetic field, and U_{EW}^P is field-aligned integrated conductivity weighted zonal wind. During nighttime the disturbance dynamo induces westward winds at low latitudes. Thus, it positively contributes to provide upward electric field through dynamo wind effect.

The last term in the right hand side of equation (1) is the field arising from the vertical Pedersen current, $J_V = E_V \sum_P$, which results from the divergence of horizontal Pedersen currents. The zonal current divergence is mainly caused by the longitudinal/spatial gradients in the conductivity or ionization density. $\text{Div} J = 0$ where J is the summation of east-west (J_{EW}) and vertical (J_V) Pedersen currents. $J_{EW} = E_{EW} \sum_P$. For E_{EW} remaining constant with height and E_V holding the zero values at the base of the ionosphere at ~ 90 km, E_V along the heights l ($l > 90$) km can be expressed as

$$E_{V(\text{iii})} = -E_{EW} \int_{90}^l \frac{1}{\sum_P} \frac{d}{dx} \sum_P dl \quad (2)$$

$E_{V(\text{iii})}$ represents field contribution from the third term. We evaluate here $E_{V(\text{iii})}$ using the IRI-2012 parameters and storm time disturbance zonal electric field shown in Figure 3b. First, the conductivity gradient over spatial separation of $\pm 1^\circ$ around 77°E longitude is calculated using the parameters derived from the IRI. The height integration is performed over equatorial height range of ~ 100 km (Abdu et al., 1998). Incidentally, the estimated $E_{V(\text{iii})}$ is ~ 1.06 mV/m (upward).

Patra et al. (2016) reported a highly confined generation of equatorial spread- F irregularities over the Indian low latitude region during this storm. Based on their report and by knowing the fact that plasma bubble irregularities align along the geomagnetic field lines, we believe that in addition to the disturbance dynamo wind effects (second term in equation (1)) the spatial gradient between the field aligned Pedersen conductivity over the longitudes with equatorial spread- F irregularity and that of the void of irregularity causes significant contribution, through $E_{V(\text{iii})}$, into E_V in the present case. From the total contribution of first, second, and third terms, it is noticed that the second and third terms play crucial role in manifesting net upward vertical field over the equator.

Bagiya et al. (2017) mentioned the 17 March 2015 storm as the two-step main phase storm and discussed the dayside low latitude ionospheric response to the storm time varying electric fields during the main phase step-I of this storm. Huang et al. (2016) mentioned about the temporary recovery in SYM-H, where minimum SYM-H of ~ -101 nT recovered to -38 nT during the main phase step-I. The IMF B_z is observed to be northward during this period (Figure 1 of Huang et al., 2016). Sau et al. (2017) reported the westward drift reduction during this period as measured by the imager and attributed it to this temporary SYM-H recovery. Our observations also demonstrate the reduction in westward zonal plasma drift and its eastward turning at $\sim 18:00$ UT for a short period of time. The zonal drift again turned westward at $\sim 18:15$ UT and continued till 20:15 UT as recorded by CADI. We corroborate with Sau et al. (2017) and suggest that the weakening of westward drift in the premidnight period is due to the recovery process of main phase step-I before the initiation of the step-II. It is also suggested, here, that the commencement

of main phase step-II resurges the disturbance wind dynamo, which on its arrival at low latitudes causes the westward drift till 20:20 UT.

5. Conclusion

The present study reports the rare observation of simultaneous nocturnal downward and westward equatorial plasma drifts during the 17 March 2015 geomagnetic storm. While the vertical plasma drift variations are understood in terms of the competing effects between storm time PPE field, DDE field, and substorm associated field, the zonal plasma drift is observed to be mainly controlled by the storm induced wind dynamo at low latitudes in addition to the vertical Pedersen current arising from the spatial (longitudinal) gradient between the field-aligned Pedersen conductivity. We believe that the present study could be appreciated not only in terms of reporting the peculiar nocturnal storm time equatorial plasma drift behavior but also for understanding the distinctive effects of storm time electric fields and storm induced local electrodynamic changes over the low latitudes.

Acknowledgments

The authors are grateful to the technical staff at EGRL, Tirunelveli, for the continuous operation and maintenance of GNSS scintillation receivers and CADI experiments. We thank B.I. Panchal for extending the help during the formulation of this paper. The authors acknowledge the use of SuperDARN data. SuperDARN is a collection of radars funded by national scientific funding agencies of Australia, Canada, China, France, Japan, South Africa, United Kingdom, and the United States. The authors duly acknowledge the ACE, SWEPAM, and ACE MAG instrument team for providing solar wind and interplanetary data. The World Data Centre for Geomagnetism at Kyoto University is acknowledged for providing AU and AL data. This work is supported by Department of Science and Technology (DST), India. The scintillation receiver data are available with M.S. B., and the CADI data are available with S.S. The authors are grateful to the reviewers and the Editor for constructive comments.

References

- Abdu, M. A., Jayachandran, P. T., MacDougall, J., Cecile, J. F., & Sobral, J. H. A. (1998). Equatorial F region zonal plasma irregularity drifts under magnetospheric disturbances. *Geophysical Research Letters*, *25*(22), 4137–4140. <https://doi.org/10.1029/1998GL900117>
- Ahn, B. H., Robinson, R. M., Kamide, Y., & Akasofu, S. I. (1983). Electric conductivities, electric fields and auroral particle energy injection rate in the auroral ionosphere and their empirical relations to the horizontal magnetic disturbances. *Planetary and Space Science*, *31*, 641–653.
- Astafyeva, E., Zakharenkova, I., & Forster, M. (2015). Ionospheric response to the 2015 St. Patrick's Day storm: A global multi-instrumental overview. *Journal of Geophysical Research: Space Physics*, *120*, 9023–9037. <https://doi.org/10.1002/2015JA021629>
- Bagiya, M. S., Iyer, K. N., Joshi, H. P., Thampi, S. V., Tsugawa, T., Ravindran, S., et al. (2011). Low-latitude ionospheric response to storm time electrodynamic coupling between high and low latitudes. *Journal of Geophysical Research*, *116*, A01303. <https://doi.org/10.1029/2010JA015845>
- Bagiya, M. S., Sridharan, R., Sunda, S., Jose, L., Pant, T. K., & Choudhary, R. (2015). Impact of the perturbation zonal velocity variation on the spatio/temporal occurrence pattern of L band scintillation—A case study. *Journal of Geophysical Research: Space Physics*, *120*, 5882–5889. <https://doi.org/10.1002/2015JA021322>
- Bagiya, M. S., Sunil, A. S., Chakrabarty, D., & Sunda, S. (2017). Salient features of the dayside low latitude ionospheric response to the main phase step-I of the 17 March 2015 geomagnetic storm. *Advances in Space Research*, *60*(8), 1827–1837. <https://doi.org/10.1016/j.asr.2017.06.010>
- Bahera, J. K., Sinha, A. K., Vichare, G., Bhaskar, A., Honary, F., Rawat, R., & Singh, R. (2017). Enhancement and modulation of cosmic noise absorption in the afternoon sector at sub-auroral location ($L = 5$) during the recovery phase of 17th March 2015 geomagnetic storm. *Journal of Geophysical Research: Space Physics*, *122*, 9528–9544. <https://doi.org/10.1002/2017JA024226>
- Bhaskar, A., & Vichare, G. (2013). Characteristics of penetration electric fields to the equatorial ionosphere during southward and northward IMF turnings. *Journal of Geophysical Research: Space Physics*, *118*, 4696–4709. <https://doi.org/10.1002/jgra.50436>
- Blanc, M., & Richmond, A. D. (1980). The ionospheric disturbance dynamo. *Journal of Geophysical Research*, *85*(A4), 1669–1688. <https://doi.org/10.1029/JA085iA04p01669>
- Burke, W. J. (2007). Penetration electric fields: A Volland-Stern approach. *Journal of Atmospheric and Solar-Terrestrial Physics*, *69*, 1114–1126.
- Carter, B. A., Yizengaw, E., Pradipta, R., Retterer, J. M., Groves, K., Valladares, C., et al. (2016). Global equatorial plasma bubble occurrence during the 2015 St. Patrick's Day storm. *Journal of Geophysical Research: Space Physics*, *121*, 894–905. <https://doi.org/10.1002/2015JA022194>
- Chakrabarty, D., Hui, D., Rout, D., Sekar, R., Bhattacharyya, A., Reeves, G. D., & Ruohoniemi, J. M. (2017). Role of IMF B_y in the prompt electric field disturbances over equatorial ionosphere during a space weather event. *Journal of Geophysical Research: Space Physics*, *122*, 2574–2588. <https://doi.org/10.1002/2016JA022781>
- Fejer, B. G. (1993). F region plasma drift over Arecibo: Solar cycle, seasonal, and magnetic activity effects. *Journal of Geophysical Research*, *98*(A8), 13,645–13,652. <https://doi.org/10.1029/93JA00953>
- Fejer, B. G., & Emmert, J. T. (2003). Low-latitude ionospheric disturbance electric field effects during the recovery phase of the 19–21 October 1998 magnetic storm. *Journal of Geophysical Research*, *108*(A12), 1454. <https://doi.org/10.1029/2003JA010190>
- Fejer, B. G., Jensen, J. W., Kikuchi, T., Abdu, M. A., & Chau, J. L. (2007). Equatorial ionospheric electric fields during the November 2004 magnetic storm. *Journal of Geophysical Research*, *112*, A10304. <https://doi.org/10.1029/2007JA012376>
- Fejer, B. G., Larsen, M. F., & Farley, D. T. (1983). Equatorial disturbance dynamo electric fields. *Geophysical Research Letters*, *10*(7), 537–540. <https://doi.org/10.1029/GL010i007p00537>
- Greenwald, R. A., Baker, K. B., Dudeney, J. R., Pinnock, M., Jones, T. B., Thomas, E. C., et al. (1995). DARN/SuperDARN: A global view of the dynamics of high-latitude convection. *Space Science Reviews*, *71*, 761–796.
- Haerendel, G., Eccles, J. V., & Cakir, S. (1992). Theory of modeling the equatorial evening ionosphere and the origin of the shear in the horizontal plasma flow. *Journal of Geophysical Research*, *97*(A2), 1209–1223. <https://doi.org/10.1029/91JA02226>
- Huang, C., Sazykin, S., Chau, J. L., Maruyama, N., & Kelley, M. C. (2007). Penetration electric fields: Efficiency and characteristic time scale. *Journal of Atmospheric and Solar - Terrestrial Physics*, *69*(10-11), 1135–1146. <https://doi.org/10.1016/j.jastp.2006.08.016>
- Huang, C. M., Chen, M. O., & Su, S. Y. (2008). Plasma drift observations associated with intense magnetic storms by the IPEI on board ROCSAT-1. *Journal of Geophysical Research*, *113*, A11301. <https://doi.org/10.1029/2008JA013405>
- Huang, C. M., Chen, M. Q., & Liu, J. Y. (2010). Ionospheric positive storm phases at the magnetic equator close to sunset. *Journal of Geophysical Research*, *115*, A07315. <https://doi.org/10.1029/2009JA014936>
- Huang, C.-S., Wilson, G. R., Hairston, M. R., Zhang, Y., Wang, W., & Liu, J. (2016). Equatorial ionospheric plasma drifts and O⁺ concentration enhancements associated with disturbance dynamo during the 2015 St. Patrick's Day magnetic storm. *Journal of Geophysical Research: Space Physics*, *121*, 7961–7973. <https://doi.org/10.1002/2016JA02307>

- Iyer, K. N., Jivani, M. N., Abdu, M. A., Joshi, H. P., & Aggarwal, M. (2006). Power spectral studies of VHF ionospheric scintillations near the crest of the equatorial anomaly in India. *Indian Journal of Radio & Space Physics*, 35, 234–241.
- Kalita, B. R., Hazarika, R., Kakoti, G., Bhuyan, P. K., Chakrabarty, D., Seemala, G. K., et al. (2016). Conjugate hemisphere ionospheric response to the St. Patrick's Day storms of 2013 and 2015 in the 100°E longitude sector. *Journal of Geophysical Research: Space Physics*, 121, 11,364–11,390. <https://doi.org/10.1002/2016JA023119>
- Kamide, Y., & Kusano, K. (2015). No major solar flares but largest geomagnetic storm in the present solar cycle. *Space Weather*, 13, 365–367. <https://doi.org/10.1002/2015SW001213>
- Kataoka, R., Shiota, D., Kilpua, E., & Keika, K. (2015). Pileup accident hypothesis of magnetic storm on 17 March 2015. *Geophysical Research Letters*, 42, 5155–5161. <https://doi.org/10.1002/2015GL064816>
- Kelley, M. C., Fejer, B. G., & Gonzales, C. A. (1979). An explanation for anomalous equatorial ionospheric electric field associated with a northward turning of the interplanetary magnetic field. *Geophysical Research Letters*, 6, 301–304.
- Kelley, M. C., Makela, J. J., Chau, J. L., & Nicholls, M. J. (2003). Penetration of the solar wind electric field into the magnetosphere/ionosphere system. *Geophysical Research Letters*, 30(4), 1158. <https://doi.org/10.1029/2002GL016321>
- Kelley, M. C., & Retterer, J. (2008). First successful prediction of a convective equatorial ionospheric storm using solar wind parameters. *Space Weather*, 6, S08003. <https://doi.org/10.1029/2007SW000381>
- Liu, J., Wang, W., Burns, A., Yue, X., Zhang, S., Zhang, Y., & Huang, C. (2016). Profiles of ionospheric storm-enhanced density during the 17 March 2015 great storm. *Journal of Geophysical Research: Space Physics*, 121, 727–744. <https://doi.org/10.1002/2015JA021832>
- Nava, B., Rodriguez-Zuluaga, J., Alazo-Cuartas, K., Kashcheyev, A., Migoya-Orue, Y., Radicella, S. M., et al. (2016). Middle- and low-latitude ionosphere response to 2015 St. Patrick's Day geomagnetic storm. *Journal of Geophysical Research: Space Physics*, 121, 3421–3438. <https://doi.org/10.1002/2015JA022299>
- Nishida, A. (1968). Coherence of geomagnetic DP 2 fluctuations with interplanetary magnetic field variations. *Journal of Geophysical Research*, 73(17), 5549–5559. <https://doi.org/10.1029/JA073i017p05549>
- Patra, A. K., Chaitanya, P. P., Dashora, N., Sivakandan, M., & Taori, A. (2016). Highly localized unique electrodynamic and plasma irregularities linked with the 17 March 2015 severe magnetic storm observed using multitechnique common-volume observations from Gadanki, India. *Journal of Geophysical Research: Space Physics*, 121, 11,518–11,527. <https://doi.org/10.1002/2016JA023384>
- Ramsingh, Sripathi, S., Sreekumar, S., Banola, S., Emperumal, K., Tiwari, P., & Kumar, B. S. (2015). Low-latitude ionosphere response to super geomagnetic storm of 17/18 March 2015: Results from a chain of ground-based observations over Indian sector. *Journal of Geophysical Research: Space Physics*, 120, 10,864–10,882. <https://doi.org/10.1002/2015JA021509>
- Ray, S., Roy, B., Paul, K. S., Goswami, S., Oikonomou, C., Haralambous, H., et al. (2017). Study of the effect of 17–18 March 2015 geomagnetic storm on the Indian longitudes using GPS and C/NOFS. *Journal of Geophysical Research: Space Physics*, 122, 2551–2563. <https://doi.org/10.1002/2016JA023127>
- Sau, S., Narayanan, V. L., Gurubaran, S., Ghodpage, R. N., & Patil, P. T. (2017). First observation of interhemispheric asymmetry in the EPBs during the St. Patrick's Day geomagnetic storm of 2015. *Journal of Geophysical Research: Space Physics*, 122, 6679–6688. <https://doi.org/10.1002/2017JA024213>
- Scherliess, L., & Fejer, B. G. (1997). Storm time dependence of equatorial disturbance dynamo zonal electric fields. *Journal of Geophysical Research*, 102(A11), 24,037–24,046. <https://doi.org/10.1029/97JA02165>
- Sripathi, S., Singh, R., Banola, S., Sreekumar, S., Emperumal, K., & Selvaraj, C. (2016). Characteristics of the equatorial plasma drifts as obtained by using Canadian Doppler ionosonde over southern tip of India. *Journal of Geophysical Research: Space Physics*, 121, 8103–8120. <https://doi.org/10.1002/2016JA023088>
- Vichare, G., Ridley, A., & Yigit, E. (2012). Quiet-time low latitude ionospheric electrodynamic in the non-hydrostatic Global Ionosphere–Thermosphere Model. *Journal of Atmospheric and Solar - Terrestrial Physics*, 80, 161–172.
- Zakharenkova, I., Astafyeva, E., & Cherniak, I. (2016). GPS and GLONASS observations of large-scale traveling ionospheric disturbances during the 2015 St. Patrick's Day storm. *Journal of Geophysical Research: Space Physics*, 121, 12,138–12,156. <https://doi.org/10.1002/2016JA023332>
- Zhang, S.-R., Erickson, P. J., Foster, J. C., Holt, J. M., Coster, A. J., Makela, J. J., et al. (2015). Thermospheric poleward wind surge at midlatitudes during great storm intervals. *Journal of Geophysical Research: Space Physics*, 42, 5132–5140. <https://doi.org/10.1002/2015GL064836>
- Zhong, J., Wang, W., Yue, X., Burns, A. G., Dou, X., & Lei, J. (2016). Long-duration depletion in the topside ionospheric total electron content during the recovery phase of the March 2015 strong storm. *Journal of Geophysical Research: Space Physics*, 121, 4733–4747. <https://doi.org/10.1002/2016JA022469>